

Thermal Behavior of Tetrahydropyran-Intercalated VOPO₄: Structural and Dynamics Study

Klára Melánová,^[a] Ludvík Beneš,^{*[a]} Vítězslav Zima,^[a] Eva Černošková,^[a] Jiří Brus,^[b] Martina Urbanová,^[b] Miroslava Trchová,^[b] and Jiří Dybal^[b]

Keywords: Intercalations / NMR spectroscopy / IR spectroscopy / Thermal behavior / Quantum chemical calculations

The thermal behavior of tetrahydropyran-(THP-)intercalated VOPO₄ was probed by an extensive combination of experimental methods (XRD, DSC, FTIR, solid-state NMR) and quantum chemical calculations. Two temperature-induced transitions were detected and all polymorphs exhibit a high degree of molecular order and tight packing of THP in VOPO₄. The first reversible thermal transition at around 100 °C was attributed to boat/chair conformation changes of the THP molecules. Most probably, a low-temperature boat conformation of the guest molecules present in the interlayer space of VOPO₄ changes to a high-temperature chair confor-

mation. This rearrangement of the THP molecules was confirmed by variable-temperature ¹³C CP/MAS NMR spectroscopy. Quantum chemical calculations using a B3LYP functional and 6-31G(d) basis set also support this idea. The second change at around 140 °C is probably caused by a weakening of the donor–acceptor bond between the oxygen molecule of THP and the vanadium atom of the host and the formation of a disorder in packing of the THP molecules.

(© Wiley-VCH Verlag GmbH & Co. KGaA, 69451 Weinheim, Germany, 2007)

Introduction

Vanadyl phosphate belongs to phosphates with a layered structure. The layers are formed of a tetragonal grid in which atoms of vanadium and phosphorus alternate. The atoms of vanadium and phosphorus are connected by oxygen atoms (O_{host}) of the phosphate groups.^[1,2]

Thus, every vanadium atom is surrounded by four equatorial oxygen atoms. In addition, two oxygen atoms are bonded to the vanadium atoms forming a VO₆ octahedron. One of these two vanadium–oxygen bonds is shorter indicating the presence of a V=O bond, while the other is much longer and can be ascribed to the coordination of the oxygen atom from the V=O group of an adjacent (VOPO₄)_∞ layer. The interlayer interactions are therefore accomplished by V=O...V bonds in anhydrous VOPO₄. In the vanadyl phosphate intercalates, the sixth position in the VO₆ octahedron is complemented by a donor atom of a guest molecule, which is then in a *trans* position to the oxygen atom of the V=O bond. Vanadyl phosphate forms a number of intercalation compounds with molecular guests having Lewis base character, among others also with ether oxygen as a donor atom.^[3] Recently, tetrahydrofuran,^[4,5] tetrahydropyran (THP),^[5] 1,4-dioxane, 1,3,5-trioxane, and 18-crown-6^[6]

were intercalated into vanadyl phosphate. It is presumed that the guests are coordinated to the vanadium atoms of the host layer through the free electron pairs of the donor O atoms of the guests. These intercalates are generally very stable in air and the guest molecules are released at relatively high temperatures (for example the tetrahydrofuran intercalate decomposes at about 160 °C^[5]). This indicates that the host–guest interaction is very strong.

Recently, we studied the thermal behavior of tetrahydropyran-intercalated VOPO₄. This intercalate was prepared by replacing 1-propanol in the VOPO₄·2C₃H₇OH intercalate with the THP. The lattice parameters of the tetragonal structure are *a* = 6.201(2) Å and *c* = 12.014(2) Å and the intercalate contains one THP molecule per formula unit. The probable arrangement of the THP molecules in the host interlayer space is derived from molecular simulations with the Cerius^[2] 4.5 programme. The molecular simulations showed a bilayer arrangement of the THP molecules in the interlayer space, in which the guest layers are slightly overlapping.^[5]

The thermal behavior of THP intercalated vanadyl phosphate was monitored by powder X-ray diffraction and TG-DTA. The basal spacing slightly increases up to 85 °C. At this temperature, a new phase with the basal spacing 12.8 Å appears. This effect is fully reversible during cooling. Another weak increase of the basal spacing up to 122 °C is followed by a significant increase of the basal spacing between 122–140 °C, which is accompanied by a broadening of the (00*l*) diffraction lines. At higher temperatures, the intensity of the (00*l*) diffraction lines decreases due to slow

[a] Joint Laboratory of Solid State Chemistry of Institute of Macromolecular Chemistry of Academy of Sciences and University of Pardubice, Studentská 84, 53210 Pardubice, Czech Republic

[b] Institute of Macromolecular Chemistry, Academy of Sciences of the Czech Republic, Heyrovský Sq. 2, 16206 Prague 6, Czech Republic

decomposition of the intercalate. The *a* parameter of the tetragonal lattice does not change up to 158 °C. The color of the intercalate does not change up to 122 °C at which point it changes to yellow-green. This indicates gradual reduction of vanadium(V).

As follows from the TG measurement, thermal decomposition of the intercalate starts at 140 °C, and THP is slowly released up to 600 °C. There are two endothermic effects on the DTA curve which occur at the temperatures (78 and 126 °C) when the step changes of the basal spacing are observed. No weight loss accompanies these effects. The exothermic effects at higher temperatures are probably due to the combustion of the released compounds.

The question is, what is the reason for the reversible effects that occur in the temperature range 60–130 °C and how these effects are connected to the presumed changes in the arrangement of the guest molecules in the interlayer space of the host. For this purpose, we utilized solid-state NMR spectroscopy together with other methods. Structural changes occurring in the investigated materials, in our case in the intercalated systems, can be easily inferred from the chemical shifts obtained by solid-state NMR spectroscopy. Besides, many NMR parameters are highly sensitive to the internal dynamics of molecular systems and for instance motional amplitudes of molecular segments can be directly extracted from the precise measurements of the site-specific motionally averaged one-bond dipolar couplings.

This paper reports the results of a DSC, IR, and NMR study of the thermal behavior of the THP intercalate. We focused also on the description of the basic structural motifs and motional states of the intercalated molecules of THP within the interlayer space of VOPO₄. For this task we used the analysis of the ¹³C CP/MAS NMR spectra and the measurements of the ¹H-¹³C and ¹H-³¹P dipolar coupling constants. Furthermore, the conformational changes and the rearrangement of THP molecules that occur as the temperature is gradually elevated were probed by a variable-temperature measurement of the ¹³C CP/MAS NMR spectra.

Results and Discussion

The THP intercalate was prepared according to two methods: stirring at room temperature and refluxing. Both methods provide samples with the same composition VOPO₄·C₅H₁₀O but with slightly different basal spacings. The sample prepared at room temperature has a basal spacing of 12.02 Å and its lattice parameters are the same as those of the intercalate described in the previous paper.^[5] The sample prepared by refluxing has a slightly higher basal spacing of 12.11 Å. Both samples were heated to 115 °C and then cooled to room temperature. After the thermal treatment, the basal spacing of the sample prepared at room temperature shifts from 12.02 to 12.11 Å (see Figure 1a). On the other hand, the diffractograms of the sample prepared by refluxing are practically the same before

and after the thermal treatment and its thermal XRD behavior seems to be fully reversible (Figure 1b). Therefore, all other investigations were done with this sample.

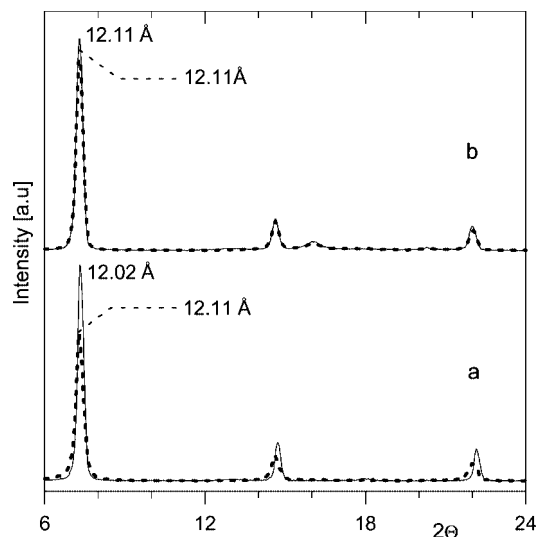


Figure 1. Comparison of the diffractograms measured before (solid line) and after (dashed line) thermal treatment for the THP intercalate prepared at room temperature (a) and by refluxing (b).

DSC Measurements

Figure 2 shows the DSC curves for the intercalate. Three cycles of heating and cooling were carried out (curves 1–6). The first heating curve (dashed line 1) shows an endothermic peak at 98 °C with a shoulder at 102 °C. The second and third heating curves (3 and 5) are identical and differ

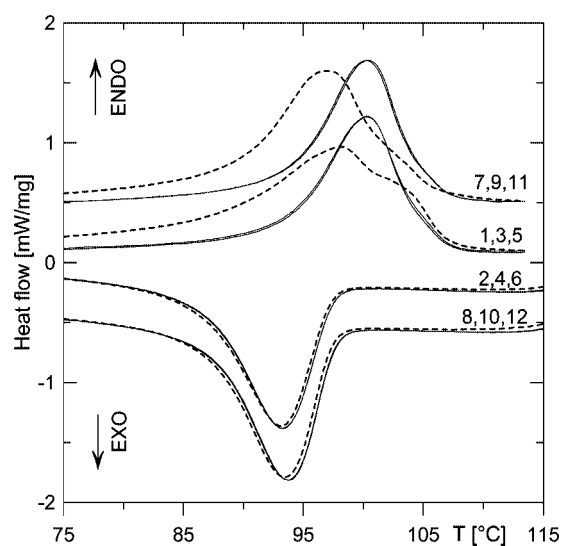


Figure 2. DSC curves of the intercalate prepared by refluxing. The curves are numbered as they were measured. The measurements 7–12 were repeated after 5 d with the same samples as measurements 1–6. The first cycles of heating (1 and 7) and cooling (2 and 8) are marked with dashed lines.

from the first heating curve. They have only one endothermic peak at 100.5 °C. All three cooling curves (2, 4, and 6) are nearly the same.

After 5 d, another three heating and cooling cycles were carried out with the same sample. The first heating curve in this series (dashed line 7) is similar to the first heating curve of the fresh sample. There is an endothermic peak at 97 °C but the shoulder at 102 °C is less marked. It indicates some slow relaxation at room temperature. The next two heating curves (9 and 11) and all cooling curves (8, 10, and 12) are practically the same and do not differ from those of the fresh sample.

FTIR Spectroscopy

The phase transitions in $\text{VOPO}_4 \cdot \text{C}_5\text{H}_{10}\text{O}$ intercalate demonstrated by DSC analysis have been tested by FTIR spectroscopy. The FTIR spectra of the intercalate $\text{VOPO}_4 \cdot \text{C}_5\text{H}_{10}\text{O}$ during heating from 25 to 120 °C and of pure THP are shown in Figures 3 and 4.

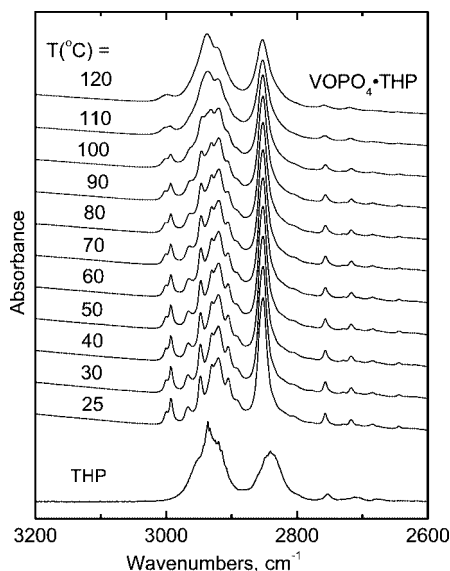


Figure 3. FTIR spectra of the intercalate VOPO_4 with THP in KBr pellets during heating from 25–120 °C and ATR FTIR spectrum of pure THP in the region from 3200 to 2600 cm^{-1} .

The infrared spectrum of the $\text{VOPO}_4 \cdot \text{C}_5\text{H}_{10}\text{O}$ intercalate at ambient temperature exhibits pronounced peaks which correspond to the THP vibrations. The intercalation of THP into vanadyl phosphate has been characterized by IR and Raman spectroscopy.^[5] The band at 996 cm^{-1} in the infrared spectrum of $\text{VOPO}_4 \cdot \text{C}_5\text{H}_{10}\text{O}$ has been assigned to the symmetric $\nu(\text{PO}_4)$ stretching vibration which is infrared-active due to the distortion of the phosphate tetrahedron in the intercalate. The shoulder at 1001 cm^{-1} is most probably the $\text{V}=\text{O}$ stretching band of the vanadyl group. Its position corresponds to the coordination of the oxygen atom of THP to the other axial position of the VO_6 octahedron. The band at 1149 cm^{-1} in the infrared spectrum of the in-

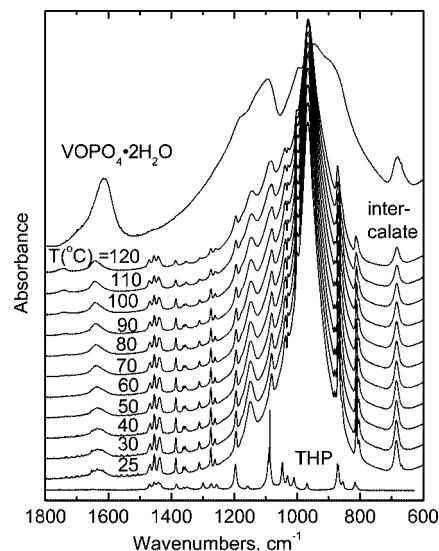


Figure 4. FTIR spectra of $\text{VOPO}_4 \cdot \text{H}_2\text{O}$ and of the intercalate VOPO_4 with THP in KBr pellets during heating from 25 to 120 °C and ATR FTIR spectrum of pure THP in the region from 1800 to 600 cm^{-1} .

tercalate with THP is the asymmetric $\nu(\text{PO}_4)$ stretching vibration of the phosphate tetrahedron. The position of the main spectral bands of the host structure differs only slightly from those of anhydrous vanadyl phosphate or its hydrated form.^[7] This confirms that the structure of the original VOPO_4 layers remains unchanged after the intercalation reaction.

The position, shape, and intensity of bands in the 3100–2700 cm^{-1} region (see Figure 3) of the spectrum of the intercalate differs from those in the spectrum of pure THP.^[8,9] Some changes of the CH_2 stretching vibrations have been observed when going from the liquid state to the intercalated form of THP. During the fixation of the intercalated molecules in the interlayer space, the asymmetric CH_2 stretching vibrations at 2936 and 2840 cm^{-1} split into several bands and a new doublet shifted to 3002 and 2993 cm^{-1} appears in the infrared spectrum of the intercalated THP (see Figure 3). Going from the liquid to the intercalated state of THP a change of the scissoring (several bands from 1380 to 1470 cm^{-1}), wagging (at about 1350 cm^{-1}), twisting (at about 1250 cm^{-1}), and rocking (at about 1150 cm^{-1}) vibrations of the CH_2 group have been observed in the infrared spectrum of the intercalate (see Figure 4).^[8,9] The band of the asymmetric $\text{C}-\text{O}-\text{C}$ ring vibrations at about 1090 cm^{-1} is overlapped by PO_4 vibrations of vanadyl phosphate in the infrared spectrum. The position of the deformation ring vibration is shifted from 817 to 813 cm^{-1} in the infrared spectrum. The peak of the deformation ring vibration at 872 cm^{-1} of THP is shifted to 870 cm^{-1} with a shoulder at 881 cm^{-1} .

The infrared spectra of the VOPO_4 intercalate with THP present some reversible changes during heating to 120 °C and cooling back to 25 °C. In the region 3100–2700 cm^{-1} , the asymmetric CH_2 stretching vibration, which is split into

several bands at ambient temperature, passes to two bands at 2936 and 2840 cm⁻¹ and the doublet at 3002 and 2993 cm⁻¹ passes to one band at 3001 cm⁻¹ during heating at about 110 °C. This transition occurs at 90 °C during cooling (see Figure 3). At the same temperatures we observe the reversible changes in the region from 1500 to 1100 cm⁻¹ of the scissoring, wagging, and twisting vibrations of CH₂ groups and in the region from 1000 to 800 cm⁻¹ of the ring deformation vibration (see Figure 4). The observed changes might be explained by the existence of two different conformations of the intercalated THP molecules. Basically, a six-membered ring of THP can adopt one of the two most common conformations: boat and chair. At ambient temperature, the attractive forces between the host layers compel the guest molecules to adopt the boat conformation, which is spatially less demanding. The corresponding low-temperature intercalate has therefore a lower basal spacing. On heating, the attractive forces between layers become less important and the THP molecule can adopt the energetically most favorable conformation, the chair conformation. The high-temperature chair conformation requires more space which results in a higher basal spacing of the intercalate at elevated temperature. This idea is strongly supported by the quantum mechanical calculations presented below.

NMR Spectroscopy

Local Structure and Segmental Dynamics

The standard ¹³C CP/MAS NMR spectrum of the intercalate (Figure 5a) clearly reflects that the THP molecules intercalated between the layers of vanadyl phosphate are regularly arranged. This is indicated by relatively narrow and symmetric signals with a linewidth of about 0.59, 0.55, and 0.45 ppm for signals C1, C2, and C3, respectively. As these linewidths are almost comparable with the linewidths of CH₂ signals of highly crystalline substances measured under the same conditions (e.g. glycine: 0.42 ppm), this feature reflects a high degree of organization and packing of the THP molecules. The other possible explanation, a narrowing of the signals due to the fast rotation or fast ring interconversion of the THP molecules in the interlayer space, can be excluded. As reflected by the determined heteronuclear one-bond ¹H-¹³C dipolar splitting ν_{CH} = 12.2–11.8 kHz (Figure 6), the THP molecules in the basic state at room temperature are fairly immobilized. This follows from the comparison with the expected rigid limit value of ν_{CH} , found to be 12.3 kHz based on a model compound measurement (crystalline glycine).

Motional averaging of the dipolar splitting expressed by an order parameter^[10]

$$S = \nu_{CH}/\nu_{CH,rig} = \nu_{CH}/12.3 \text{ kHz}$$

is a measure of the equilibrium distribution of orientations of the bond vector in a molecular reference frame. Assuming segmental motion to be axially symmetric and small in amplitude ($\langle \sin \theta \rangle \approx \langle \theta \rangle$), the order parameter can be

converted to a root mean square (*r.m.s.*) angular fluctuation of the bond vector according to the following definition:^[10,11]

$$S = 1 - \frac{3}{2} \langle \theta^2 \rangle$$

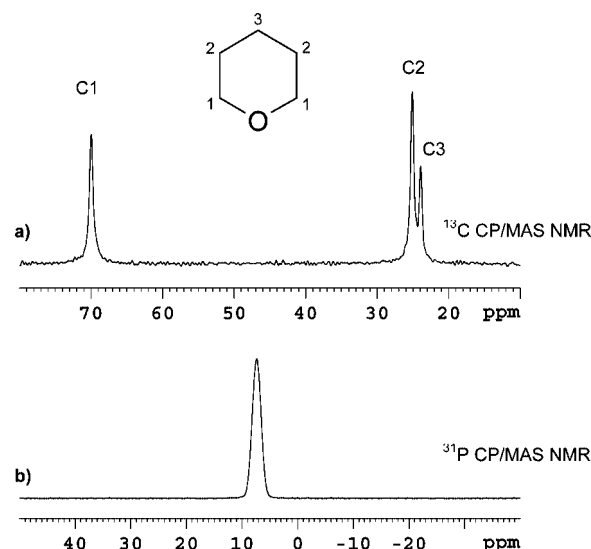


Figure 5. ¹³C CP/MAS NMR spectrum (a) and ³¹P CP/MAS NMR spectrum (b) of VOPO₄ with THP.

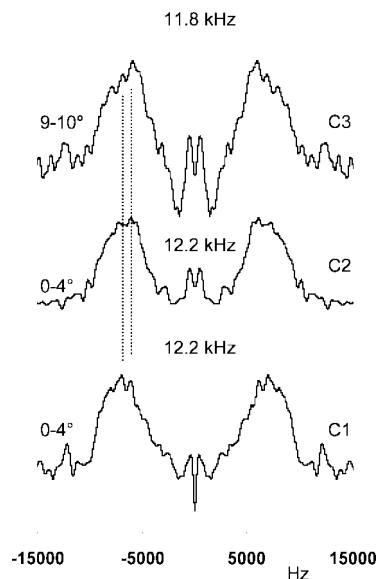


Figure 6. ¹³C{¹H} NMR dipolar spectra of CH₂ units of the intercalated THP molecules measured at room temperature. The splitting in kHz ($\Delta\nu$) reflecting the motionally averaged dipolar coupling constant (D_{CH}) is shown between the maxima and calculated *r.m.s.* amplitudes at the left side of each spectrum.

In the case of the THP molecules intercalated in VOPO₄ the order parameter *S* ranges from 0.995 to 0.959. Applying the above-mentioned simplest but still physically realistic model, the determined motional amplitudes of the most rigid carbon atoms C1 and C2 of the THP molecule are about 0–4°. The motional amplitude of the most mobile segment C3 corresponds to a fluctuation angle of about 9–10°. This definitely confirms very low flexibility of THP

molecules at room temperature and therefore existence in one preferred conformation. The observed motional restrictions are probably induced by strong interaction with VOPO_4 layers.

The character of this intermolecular binding can be deduced from the ^{13}C NMR chemical shift. At room temperature the chemical shifts for the resonance peaks of THP trapped in as-synthesized vanadyl phosphate are significantly different from those of THP in the liquid state. It can be seen that the chemical shifts of the carbon atom connected to the oxygen atom in THP (C1), move to low field ($\delta = 69.9$ ppm) in the VOPO_4 intercalate in comparison with $\delta = 68.4$ ppm in the liquid state. Oppositely, the signals of C2 are significantly moved to high field ($\delta = 25.1$ ppm), while the position of the signal of the C3 atom is almost unchanged ($\delta = 23.9$ ppm). In the liquid state the carbon atoms C2 and C3 resonate at $\delta = 26.9$ and 23.8 ppm. This phenomenon is caused by the nature of the interaction between the oxygen atom of THP and vanadyl phosphate. THP is a polar molecule in which the electronegativity of the oxygen atom is larger than that of the carbon atoms. As the oxygen atom of THP approaches the V atom, part of the electrons on the oxygen atom move to the vanadium atom, leaving the C1 atom with less negative charge. The deshielding effect causes the chemical shift to move to lower field, leading to a larger value of the chemical shift. Consequently, due to the inductive effects, electron density increases around the C2 atoms leading to a higher shielding of the nuclear spins and corresponding lower values of the chemical shifts. As the observed changes in the chemical shift are relatively large, +1.5 and -1.8 ppm for C1 and C2, respectively, the interaction between THP and the vanadyl phosphate framework must be strong.

A tight contact between the THP molecules and the VOPO_4 framework is further evidenced by a ^{31}P CP/MAS NMR experiment in which the nuclear polarization is transferred from hydrogen atoms of THP to spatially close phosphorus atoms (their distance must not exceed 6 Å). As this experiment can be easily performed (Figure 5b) and the obtained result is quite identical with the ^{31}P MAS NMR spectrum measured with a direct excitation of the ^{31}P magnetization (not shown here) the THP molecules must be regularly arranged over the whole sample and must be in close contact with all phosphorus atoms.

Average short distances between the hydrogen and phosphorus atoms were estimated from the measurement of ^{31}P - ^1H dipolar profiles employing a recently developed and applied two-dimensional Lee–Goldburg cross-polarization experiment.^[12,13] The obtained dipolar spectrum (Figure 7) probably corresponds to two superimposed dipolar doublets reflecting a superposition of two independent contributions. The most probable short-range ^1H - ^{31}P pairs are reflected by the main splitting of the dipolar spectrum which is about 210 Hz. This corresponds to the average interatomic distance of 5.1 Å. The outer low-intensive doublet with the dipolar splitting of 460 Hz may reflect the shortest ^1H - ^{31}P pairs, the interatomic distance of which is about 4.0 Å. The reliability of the applied analysis of the

^1H - ^{31}P dipolar spectrum was confirmed by the measurement and subsequent simulation of the ^1H - ^{31}P dipolar profiles for a four-spin system of CaHPO_4 for which the neutron-diffraction crystal structure is well known.^[14]

Variable-Temperature ^{13}C CPIMAS NMR Spectroscopy

Variable-temperature NMR experiments offer an interesting prospect to probe a temperature-induced rearrangement occurring in the investigated intercalated system. Gen-

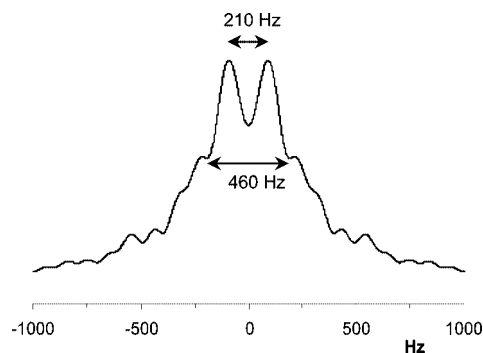


Figure 7. $^{31}\text{P}\{^1\text{H}\}$ dipolar spectrum of $\text{VOPO}_4\cdot\text{THP}$ intercalate measured at room temperature. The splitting in Hz ($\Delta\nu$) is shown between the maxima.

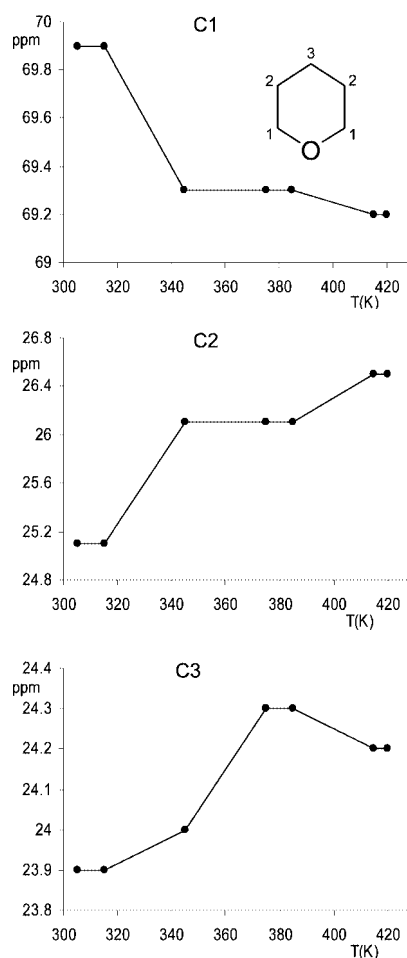


Figure 8. Temperature dependence of the ^{13}C NMR chemical shift of VOPO_4 with THP.

erally, an increase in temperature may help to overcome energy barriers and a reconstitution of the molecules – transition to another “polymorphic” form – can take place. Such changes can be simply monitored by two basic NMR parameters: chemical shift and linewidth of the ¹³C NMR signals.

In our particular case the temperature dependence of the ¹³C NMR chemical shifts (Figure 8) clearly revealed two conformation transitions. Both these transitions are not quite instant and rather occur in more or less broad temperature ranges. The first one occurs in the temperature range 70–85 °C and it is accompanied by a rearrangement of the THP molecules. This statement follows from three observed phenomena: (i) the ¹³C NMR shifts of the C1 and C2 carbons signals substantially moved; (ii) the linewidth of all signals after the transition is significantly narrowed; and finally, (iii) in the temperature range of the phase transition it is almost impossible to record the ¹³C NMR spectra.

The impossibility to detect the ¹³C NMR spectra indicates that the molecules of THP are involved in the dynamic exchange process. The molecular motion, however, is neither very fast nor isotropic, because the ¹³C MAS NMR spectrum measured with direct excitation provides only broad and unresolved signals. That is why this transformation could be attributed to the local conformation transition, for example boat/chair, which – at this temperature range – is reversible. At higher temperatures (95–130 °C)

after the first transition, the molecules of THP are again stabilized and rearranged with a significantly higher degree of self-assembling. This is reflected by a high efficiency of the cross-polarization and very narrow signals with a linewidth of 0.48–0.38 ppm (Figure 9). The second transition occurring at about 130 °C is not so dramatic. We observe only slight changes in the ¹³C NMR shift and slight broadening of the corresponding signals indicating increased disorder in packing of the THP molecules. The changes in the chemical shifts observed with increasing temperature further indicate a tendency of the molecules of THP to reach a relatively “free” state without the strong interaction with the VOPO₄ framework. Each transition is probably connected to a weakening of the intermolecular interactions between the THP molecules and vanadyl phosphate structure units.

Quantum Chemical Calculations

The character of the bonding between the guest molecules and the host layer in the THP intercalate was investigated by the methods of quantum chemical calculations. Figure 10 shows a DFT-optimized structure of the molecular segment representing local interactions of vanadyl phosphate with THP, using a B3LYP functional and 6-31G(d) basis set. In order to keep the overall planar structure of the segment during full geometry optimizations and to make the electronic structure in the segment close to the conditions appearing in the intercalates, an oxygen atom was inserted between two neighboring PO₄ groups and terminal oxygen atoms were substituted by OH groups.^[15] The

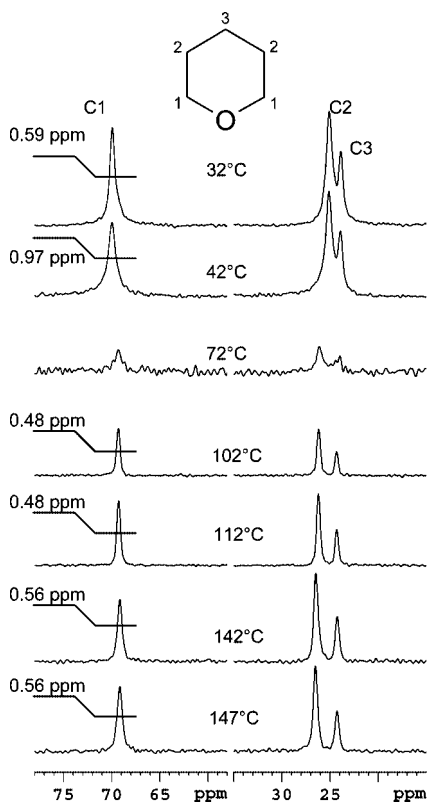


Figure 9. Variable-temperature ¹³C CP/MAS NMR spectra of VOPO₄ with THP.

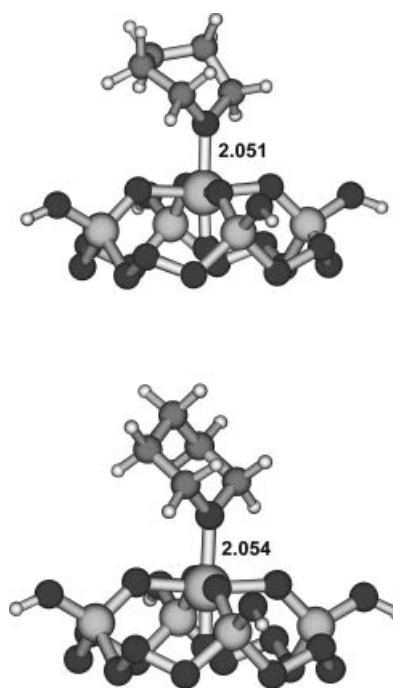


Figure 10. Optimized B3LYP/6-31G(d) structures of the molecular segment modeling the vanadyl phosphate–THP interaction with THP in boat and chair conformations.

total charge of the model compound was set to +3. It was found that all geometry optimizations with various starting orientations of THP with respect to the vanadyl group lead to the structures displayed in Figure 10, with the boat and chair conformations of THP. The structure with the chair conformation is energetically more favored by 4.9 kcal/mol.

Conclusions

In summary, the following conclusions can be made:

(i) The donor-acceptor bond between the oxygen atom of THP and the vanadium atom of VOPO_4 has been confirmed by both IR and NMR spectroscopy. This bond loosens with increasing temperature.

(ii) The phase transition observed by the DSC and powder XRD methods is accompanied with changes in the infrared spectrum of the intercalate.

(iii) The existence of two phases (with the phase transition in the temperature region 80–120 °C) could be explained by the fact that the six-membered ring of THP forms two conformations: chair and boat. The chair conformation is energetically more favorable, as follows from the quantum chemical calculations, but is sterically more demanding. Thus, its existence can be presumed at higher temperature, when there is more space between the layers of the host as indicated by higher basal spacing observed for the high-temperature phase. The boat conformation, on the other hand, can be arranged in the interlayer space in such a way that the distance between layers is lower. Therefore, this boat conformation can be present in the low-temperature phase, where it is favored by steric conditions.

(iv) The second transition/change at around 140 °C is most probably caused by weakening of the donor–acceptor bond $\text{O}_{\text{THP}}\text{--V}$ and formation of a disorder in packing of the THP molecules. These phenomena are followed by a slow decomposition of the intercalate.

Experimental Section

Sample Preparation: The THP intercalate was prepared either by stirring a suspension of $\text{VOPO}_4 \cdot 2\text{C}_3\text{H}_7\text{OH}$ in THP at room temperature overnight or by refluxing a suspension of $\text{VOPO}_4 \cdot 2\text{C}_3\text{H}_7\text{OH}$ in THP for 1 h. The products were filtered off and dried under nitrogen at room temperature.

XRD: The powder data were obtained with a D8 Advance diffractometer (Bruker AXE, Germany) using $\text{Cu-K}\alpha$ radiation with a secondary graphite monochromator. The diffraction angles were measured from 7 to 80° (2 θ). The temperature measurements from 25 to 200 °C were carried out on the heated corundum plate with a thermocouple. Each diffractogram was measured at constant temperature and each cycle of heating and measuring lasted about 60 min.

DSC Measurements: DSC experiments were performed with a Mettler DSC 12E instrument. The instrument was previously calibrated with indium, tin, and lead standards. A crystalline powder sample of about 1 mg was placed in an aluminum pan and measured with a heating and cooling rate of 5 K min^{−1} in the range from 40 to 115 °C.

Infrared Measurements: The structural and optical properties of the samples were checked using Fourier transform infrared (FTIR) spectroscopy. Infrared measurements were performed with a Bruker IFS 55 EQUINOX FTIR spectrometer with a DLATGS detector. All spectra in the range 400–4000 cm^{−1} with 2 cm^{−1} spectral resolution were obtained from compressed KBr pellets in which the $\text{VOPO}_4 \cdot \text{THP}$ powders were evenly dispersed. Two hundred scans were used to record each FTIR spectrum. A variable-temperature-controlled cell (Specac Ltd.) in the range from 0 to +250 °C with solid holders was used for temperature-dependent measurements. The spectrum of the corresponding liquid THP was measured by the ATR technique on a ZnSe crystal. The spectra were corrected for the content of H_2O and CO_2 in the optical path.

Solid-State NMR Spectroscopy: Standard one-dimensional (1D) experiments with cross-polarization (CP) and with direct excitation as well as two-dimensional (2D) recoupling experiments were performed with a Bruker Avance 500 NMR spectrometer (Karlsruhe, Germany, 2003) with a 4-mm ZrO_2 rotor. Magic-angle spinning (MAS) speed was 10–12 kHz, the nutation frequency of the $B_1(^{13}\text{C})$ and $B_1(^{31}\text{P})$ field was 62.5 kHz, and the repetition delay was 4 s. To detect site-specific ^1H – ^{13}C and ^1H – ^{31}P dipolar spectra, 2D PILGRIM (Phase Inverted LG Recoupling under MAS) experiments^[12] were applied. Incremented off-resonance LG-CP with a 22.6 μs increment was used as a dipolar evolution period. The intensity of the $B_1(^1\text{H})$ field for cross-polarization was $\omega_1/2\pi = 62.5$ kHz and Hartman–Hahn matching conditions at the +1 spinning side-band were optimized experimentally. TPPM (two-pulse phase-modulated) decoupling was applied during the detection periods. The phase modulation angle was 15°, and the flip-pulse length was 4.7 μs . The applied nutation frequency of the $B_1(^1\text{H})$ field was $\omega_1/2\pi = 89.3$ kHz. The ^{13}C scale was calibrated with glycine as the external standard ($\delta = 176.03$ ppm: low-field carbonyl signal). The ^{31}P scale was calibrated with CaHPO_4 ($\delta = -0.6$ ppm). Taking into account frictional heating of the samples during fast rotation^[16] precise temperature calibration was performed before variable-temperature experiments.

Method of Calculation: Quantum chemical calculations were carried out at the ab initio level of theory employing the Gaussian 98^[17] program package. Local interactions and structures in the intercalates of vanadyl phosphate with THP were studied at a DFT level using a B3LYP functional with a 6-31G(d) basis set.

Acknowledgments

This study was supported by the Academy of Sciences of the Czech Republic (AVOZ40500505) and Ministry of Education, Youth, and Sports of the Czech Republic (MSM0021627501). The help of the Grant Agency of the Academy of Sciences of the Czech Republic (grant IAA400500602) is also appreciated.

- [1] H. R. Tietze, *Aust. J. Chem.* **1981**, *34*, 2035–2038.
- [2] M. Tachez, F. Theobald, J. Bernard, A. W. Hewat, *Rev. Chim. Miner.* **1982**, *19*, 291–300.
- [3] J. Kalousová, J. Votinský, L. Beneš, K. Melánová, V. Zima, *Collect. Czech. Chem. Commun.* **1998**, *63*, 1–19.
- [4] K. Goubitz, P. Čapková, K. Melánová, W. Molleman, H. Schenk, *Acta Crystallogr., Sect. B* **2001**, *57*, 178–183.
- [5] V. Zima, K. Melánová, L. Beneš, M. Trchová, P. Čapková, P. Matějka, *Chem. Eur. J.* **2002**, *8*, 1703–1709.
- [6] L. Beneš, V. Zima, K. Melánová, M. Trchová, P. Čapková, B. Koudelka, P. Matějka, *Chem. Mater.* **2002**, *14*, 2788–2795.
- [7] M. Trchová, P. Čapková, K. Melánová, L. Beneš, P. Matějka, E. Uhlířová, *J. Solid State Chem.* **1999**, *148*, 197–204.

- [8] N. Bagget, S. A. Barker, A. B. Foster, R. H. Moore, D. H. Whiffen, *J. Am. Chem. Soc.* **1960**, *82*, 4565–4570.
- [9] J. M. Eyster, *Spectrochim. Acta A* **1974**, *30*, 2041–2046.
- [10] A. G. Palmer, J. Williams, A. McDermott, *J. Phys. Chem.* **1996**, *100*, 13293–13310.
- [11] D. Huster, L. Xiao, M. Hong, *Biochemistry* **2001**, *40*, 7662–7674.
- [12] M. Hong, X. Yao, K. Jakes, D. Huster, *J. Phys. Chem. B* **2002**, *106*, 7355–7364.
- [13] B. J. van Rossum, C. P. de Groot, V. Ladizhansky, S. Vega, H. J. M. de Groot, *J. Am. Chem. Soc.* **2000**, *122*, 3465–3472.
- [14] M. Catti, G. Ferraris, A. Filhol, *Acta Crystallogr., Sect. B* **1977**, *33*, 1223–1229.
- [15] V. Zima, K. Melánová, L. Beneš, M. Trchová, J. Dybal, *Eur. J. Inorg. Chem.* **2004**, 570–574.
- [16] J. Brus, *Solid State Nucl. Magn. Reson.* **2000**, *16*, 151–160.
- [17] M. J. Frisch, G. W. Trucks, H. B. Schlegel, G. E. Scuseria, M. A. Robb, J. R. Cheeseman, J. A. Montgomery Jr, T. Vreven, K. N. Kudin, J. C. Burant, J. M. Millam, S. S. Iyengar, J. Tomasi, V. Barone, B. Mennucci, M. Cossi, G. Scalmani, N. Rega, G. A. Petersson, H. Nakatsuji, M. Hada, M. Ehara, K. Toyota, R. Fukuda, J. Hasegawa, M. Ishida, T. Nakajima, Y. Honda, O. Kitao, H. Nakai, M. Klene, X. Li, J. E. Knox, H. P. Hratchian, J. B. Cross, V. Bakken, C. Adamo, J. Jaramillo, R. Gomperts, R. E. Stratmann, O. Yazyev, A. J. Austin, R. Cammi, C. Pomelli, J. W. Ochterski, P. Y. Ayala, K. Morokuma, G. A. Voth, P. Salvador, J. J. Dannenberg, V. G. Zakrzewski, S. Dapprich, A. D. Daniels, M. C. Strain, O. Farkas, D. K. Malick, A. D. Rabuck, K. Raghavachari, J. B. Foresman, J. V. Ortiz, Q. Cui, A. G. Baboul, S. Clifford, J. Cioslowski, B. B. Stefanov, G. Liu, A. Liashenko, P. Piskorz, I. Komaromi, R. L. Martin, D. J. Fox, T. Keith, M. A. Al-Laham, C. Y. Peng, A. Nanayakkara, M. Challacombe, P. M. W. Gill, B. Johnson, W. Chen, M. W. Wong, C. Gonzalez, J. A. Pople, *Gaussian 03*, Revision C.02, Gaussian, Inc., Wallingford, CT, **2004**.

Received: July 4, 2006

Published Online: November 27, 2006